NUCL SCI TECH (2020) 31:108
https://doi.org/10.1007/s41365-020-00823-5

Preliminary analysis of fuel cycle performance for a small modular heavy water-moderated thorium molten salt reactor

Ya-Peng Zhang[1,2,3] · Yu-Wen Ma[1,2,3] · Jian-Hui Wu[1,2,3] · Jin-Gen Chen[1,2,3] · Xiang-Zhou Cai[1,2,3]

Received: 28 April 2020 / Revised: 18 September 2020 / Accepted: 19 September 2020 / Published online: 6 November 2020

Abstract Heavy water-moderated molten salt reactors (HWMSRs) are novel molten salt reactors that adopt heavy water rather than graphite as the moderator while employing liquid fuel. Owing to the high moderating ratio of the heavy water moderator and the utilization of liquid fuel, HWMSRs can achieve a high neutron economy. In this study, a large-scale small modular HWMSR with a thermal power of 500 MWth was proposed and studied. The criticality of the core was evaluated using an in-house critical search calculation code (CSCC), which was developed based on Standardized Computer Analyses for Licensing Evaluation, version 6.1. The preliminary fuel cycle performances (initial conversion ratio (*CR*), initial fissile fuel loading mass, and temperature coefficient) were investigated by varying the lattice pitch (*P*) and the molten salt volume fraction (*VF*). The results demonstrate that the temperature coefficient can be negative over the range of investigated *P*s and *VF*s for both ^{233}U-Th and LEU-Th fuels. A core with a *P* of 20 cm and a *VF* of 20% is recommended for ^{233}U-Th and LEU-Th fuels to achieve a high performance of initial *CR* and fuel loading. Regarding TRU-Th fuel, a core with a smaller *P* ($\sim$ 5 cm) and larger *VF* ($\sim$ 24%) is recommended to obtain a negative temperature coefficient.

Keywords Molten salt reactor · Heavy water-moderated molten salt reactor (HWMSR) · Th-U fuel cycle

1 Introduction

Molten salt reactors (MSRs) are one of six candidates for Generation IV advanced reactor systems [1–3]. They employ heavy elements (fissile/fertile) dissolved in molten salt as fuel and coolant. The reactor system operates at a low vapor pressure but high temperature. Owing to the utilization of liquid fuel, online refueling and fission product removal are feasible for MSRs [1, 3]. These advantages not only enable MSRs to achieve higher safety and thermal conversion efficiency but also avoid periodic reactor shutdown, which might occur in the conventional solid fuel reactor while replacing fuel assemblies. In addition, the flowing liquid fuel allows MSRs to online extract ^{233}Pa, which is the intermediate nuclide in the conversion chain of ^{232}Th to ^{233}U. The loss of ^{233}U resulting from the neutron absorption of ^{233}Pa in the core can be significantly reduced. Hence, MSRs are considered to be among the most suitable reactors for thorium utilization in Generation IV nuclear reactor systems [1].

This work was supported by the Chinese TMSR Strategic Pioneer Science and Technology Project (No. XDA02010000), the National Natural Science Foundation of China (No. 11905285), the Frontier Science Key Program of the Chinese Academy of Sciences (No. QYZDY-SSW-JSC016), and the National Natural Science Foundation of China (No. 11790321).

✉ Yu-Wen Ma
mayuwen@sinap.ac.cn

✉ Jin-Gen Chen
chenjg@sinap.ac.cn

1 Shanghai Institute of Applied Physics, Chinese Academy of Sciences, Shanghai 201800, China

2 CAS Innovative Academies in TMSR Energy System, Chinese Academy of Sciences, Shanghai 201800, China

3 University of Chinese Academy of Sciences, Beijing 100049, China

In the 1960s, the Oak Ridge National Laboratory (ORNL) successfully designed and built a molten salt experimental reactor (MSRE) with a power of 8 MWth. This reactor adopted graphite as a moderator and utilized different fuels (^{235}U, ^{233}U, and Pu mixed with ^{233}U, respectively) [4]. Its successful operation verified the feasibility, reliability, and safety of MSRs [5, 6]. Subsequently, graphite-moderated MSRs have undergone a series of concept evolutions. With the intention of achieving a high Th-^{233}U conversion performance, ORNL proposed the concept of the molten salt breeder reactor (MSBR), whose breeding ratio (*BR*) could achieve 1.07 by achieving a reprocessing time (reprocessing the molten salt of the primary loop once) of 10 days [7, 8]. Graphite-moderated MSRs, however, face a potential problem of positive temperature feedback due to the neutron spectral shift propitious to ^{233}U fission over ^{232}Th neutron capture as temperatures increase [9]. There are other potential challenges such as the periodic replacement of graphite caused by neutron irradiation and the disposal of high-level radioactive graphite waste [10, 11]. To address these problems, France proposed the concept of a molten salt fast reactor (MSFR) [12–15] in which graphite was removed from the core and a negative temperature coefficient was consequently achieved. However, this design poses another problem: the loading mass of fissile material is significantly increased compared with the thermal neutron spectrum reactor due to the much smaller fission cross section of fissile nuclide in the fast neutron spectrum. Heavy water is an excellent moderator because the ratio of the macroscopic slowing down power (*MSDP*) to absorption cross sections (2100) is much higher than that of other moderators such as graphite (170) and light water (70). Meanwhile, heavy water is a liquid moderator and can be purified online and recycled. Replacing graphite with heavy water as a moderator not only improves the neutron economy but also avoids periodic replacement of the moderator. Based on this consideration, Wu et al. proposed a novel concept of a heavy water-moderated MSR (HWMSR) with a power of 1000 MWe in 2019 [16]. Because of the application of heavy water moderators and liquid fuels, HWMSR inherits the main advantages of heavy water reactors and traditional MSRs, for example, high neutron economy, feasibility for online reprocessing, and suitability for thorium utilization. HWMSR adopts ^{233}U as a fissile material to initiate and refuel the core. Its initial ^{233}U loading mass is much lower than that of MSBR, and its *BR* over 60 y is 1.073, leading to a doubling time of 12 y, which is much shorter than that of MSBR (31 y).

The Th-^{233}U fuel cycle is the premise for realizing high thorium utilization on HWMSR, but there is no available ^{233}U in nature. Using the available stockpile of fissile materials to start the reactor and produce ^{233}U is accessible for the transition to the Th-^{233}U fuel cycle. Currently, available fissile materials can be generally divided into two categories: low-enriched uranium (LEU) and transuranic (TRU) elements recycled from the spent LWR fuel [17–19]. The compositions of the two fuel types are much different, which will likely lead to a large discrepancy in fuel cycle performance. Exploring different transition strategies is an important research topic for thorium utilization in HWMSR.

Small modular reactors exhibit the advantages of modular construction, low cost, and advanced passive safety, and they can facilitate the expansion of nuclear energy to remote or isolated locations (such as deserts) [20]. It is considered as one of the most promising reactor designs for future nuclear energy development. In 2012, Trellue et al. proposed a 150 MWth Salt-cooled Modular Innovative THorium HEavy water-moderated Reactor System (SMITHERS) [21], which is a solid fuel reactor cooled by molten salt that is moderated by heavy water. Heavy water moderators can create a highly thermal neutron energy spectrum that increases the neutron economy and allows low fissile loading to become critical. They also noted that further work should consist of varying the amount of heavy water in the system or optimizing the geometry of the system to achieve more breeding. In this study, a 500 MWth large-scale small modular HWMSR (SM-HWMSR) was proposed. The preliminary fuel cycle performance metrics, including the neutron spectrum, initial conversion ratio (*CR*), initial fissile fuel loading mass, temperature coefficient, and void coefficient, were systematically analyzed for different starting fuels (^{233}U-Th, LEU-Th, TRU-Th) by varying the lattice pitches (*P*, the distance between the center of the fuel channel and the center of its adjacent fuel channel) and molten salt volume fraction (*VF*). Optimal core geometrical parameters (*P* and *VF*) for different fuels are recommended to obtain relatively high initial *CR*, low initial fissile fuel loading mass, and a negative temperature coefficient.

2 Calculation model and method

2.1 SM-HWMSR system

The LSM HWMSR is a 500 MWth single-fluid MSR that can be designed as either a Th-U breeder or converter core. The layout of the SM-HWMSR is shown in Fig. 1. It consists of the reactor core, primary and secondary heat transfer loops, a control rod system, moderator cooling system, helium bubbling system, and molten salt drain tank. During the core operation, the fission heat is removed from the core by molten salt flow. Through the heat exchangers of the primary and secondary loops, the heat is

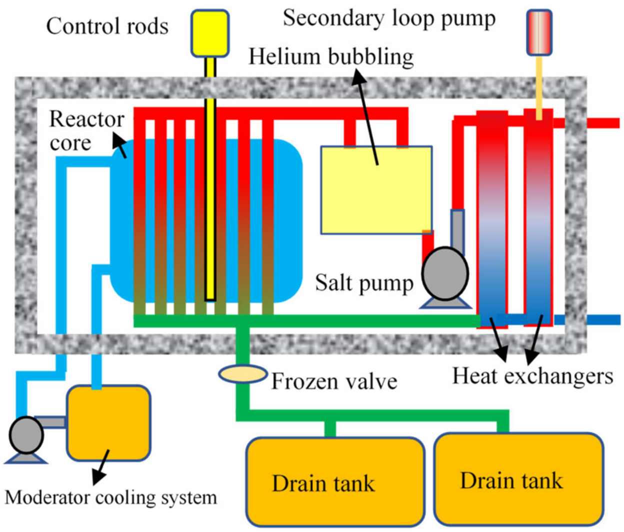

Fig. 1 (Color online) Layout of the SM-HWMSR system

finally transferred to the third loop for electricity generation. In an emergency, the control rods can be quickly inserted into the core to shut down the reactor, or the fuel salt can be quickly discharged into the drain tanks when the temperature of the fuel salt increases rapidly. A moderator cooling system was designed to remove the heat deposited in the heavy water to keep the temperature of heavy water below the boiling point at atmospheric pressure. The helium bubbling system in the primary loop is applied to remove the gaseous and noble metallic fission products by online blowing helium.

The vertical and horizontal sections of the core for SM-HWMSR, together with the enlarged view of the fuel salt cell, are presented in Fig. 2. The core is a cylindrical pool filled with heavy water. The high-temperature fuel salt continuously flows through the fuel salt conduits, which are regularly arranged in heavy water. To ensure that the temperature of the heavy water remains below the boiling point at atmospheric pressure, a thermal insulator 8YSZ-50% (8 mol% Y_2O_3/92 mol% ZrO_2 and sintered porous pellet with 50% relative density) with a thickness of 3 mm is applied to the wall of the fuel salt conduit, which can effectively maintain the temperature of heavy water below 59 °C [22]. Two 0.5-mm-thick SiC layers, which have strong corrosion-resistance and radiation-resistance in the molten salt and heavy water [23, 24], clamp the thermal insulator, forming a sandwich conduit, as shown in Fig. 2. A previous study demonstrated that the heat-insulated conduit can effectively hold back the heat transferred from the molten salt to heavy water, making the temperatures of heavy water well below the limit [16]. The main parameters of the core are summarized in Table 1. The compositions of the fuel salt are similar to that of MSBR: 71.7 mol% LiF-16 mol% BeF_2-12.3 mol% HNF_4 (chemical compound composed of heavy nuclides and fluorine). Considering the large neutron absorption cross section of ^{6}Li [25], 99.995% is taken as the ^{7}Li enrichment. The volumes of fuel salt in the core and external core were set to be 8.5 m^3 and 4 m^3, respectively. Both the height (*H*) and diameter (*D*) of the active core zone are set to be the same, and vary in a range from 3.4 m to 6.4 m by fixing the volume of molten salt in the core and changing the *VF* from 4 to 28%.

To investigate the influences of the geometrical parameters of the core (e.g., *P* and *VF*) on the fuel cycle performance, neutronic parameters including initial *CR*, initial fissile fuel loading, and temperature coefficient are analyzed by varying *P* and *VF* from 5 to 24 cm and 4% to 28%, respectively. The specific compositions of ^{233}U, LEU, and TRU are listed in Table 2. Enrichment of 19.75% is adopted for LEU considering the nonproliferation issue. The TRU is obtained by reprocessing the spent fuel discharged from the light water reactors with a burnup of 60 GWd/tons after five years of storage, which consists of Np, Pu, Am, and Cm.

2.2 Calculation method

SCALE6.1 (Standardized Computer Analyses for Licensing Evaluation, version 6.1) is a program developed by Oak Ridge National Laboratory (ORNL) for critical safety and reactor physics analysis that includes several modules. In this work, the CSAS6 (Criticality Safety

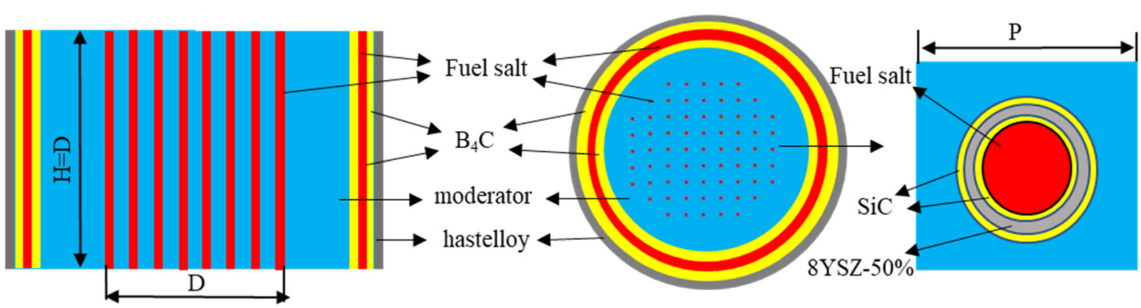

Fig. 2 (Color online) Vertical (**a**), and horizontal (**b**), sections of the core, and enlarged view of a fuel salt cell (**c**)

Table 1 Main parameters in the reactor core

Parameter	Value
Thermal power (MWth)	500
Fuel salt	
Composition (mol%)	71.7 LiF-16 BeF_2-12.3 HNF_4
^{7}Li enrichment (%)	99.995
Density (g/cm^3)	3.3
Operation temperature (°C)	630
Molten salt volume (m^3)	
Active zone	8.5
External loop	4
Heavy water moderator	
Density (g/cm^3)	1.09
Temperature (°C)	59
Diameter/height of active core (m)	3.4–6.4 (D = H)

Table 2 Starting fuel composition

Nuclide	^{233}U (%)	LEU (%)	TRU [26] (%)
U-233	100		
U-235		19.75	
U-238		80.25	
Np-237			6.23
Pu-238			2.68
Pu-239			45.77
Pu-240			21.53
Pu-241			10.77
Pu-242			6.76
Am-241			3.42
Am-243			1.92
Cm-244			0.82
Cm-245			0.1

Analysis Sequence) module, which couples the cross section processing module with the 3D Monte Carlo transport module, was used to perform the criticality calculation. The cross section library ENDF/B-VII with 238 groups was chosen.

In general, the value of the effective neutron multiplication factor k_{eff} calculated by SCALE6.1 for a given core will be larger or less than 1, which depends on core geometry and fuel compositions. Therefore, an in-house critical search calculation code (CSCC) was developed based on SCALE6.1 to search for criticality. Based on the results, the initial fissile fuel loading and initial CR can then be calculated. The main flowchart of the critical search calculation code is shown in Fig. 3. During calculation, the concentration of heavy metals in the fuel salt was maintained at 12.3 mol%. The Newton search method was adopted to search for criticality, that is, $k_{eff} = 1$, by continually adjusting the ratio of fissile fuel to thorium in heavy nuclides, and 0.0005 is taken as the deviation of the criticality search. As $|k_{eff} - 1| > 0.0005$, the ratio of fissile fuel loading mass to thorium will be adjusted through CSCC until $|k_{eff} - 1| < 0.0005$. In addition, because of the homogeneous mixing of the molten salt, the resonance self-shielding calculations are turned off when criticality calculation is performed.

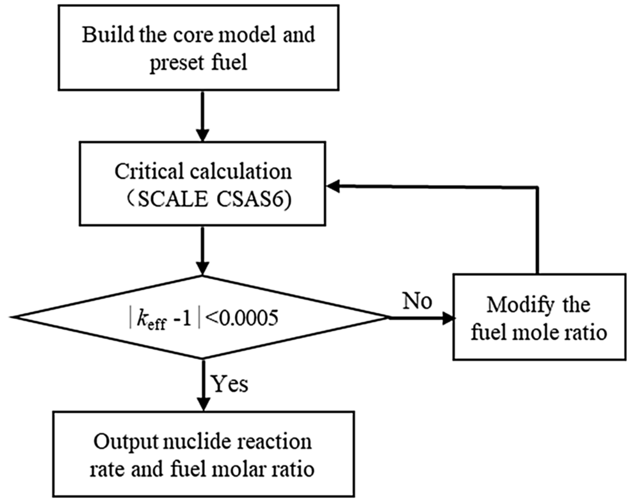

Fig. 3 Flowchart of critical search

3 Results and discussion

3.1 Influences of geometrical parameters on neutron spectrum

The uniformity of moderator arrangement (*P* value) and *VF* in the core can directly affect the ability to slow down neutrons in the core and subsequently have an impact on the neutron spectrum. However, the influence mechanism between the geometrical parameters and the neutron spectrum is still unclear. Hence, in this section, these issues are systematically investigated for each fuel type.

First, the influence of *P* on the neutron spectrum was analyzed by setting *VF* as a constant (such as 16%, typical thermal spectrum). In this case, decreasing *P* increases the number of fuel channels and reduces the radii of the fuel channels. The ratio of the fuel surface to its volume increased because the volume of molten salt is fixed. The resonance escape probability of neutrons increased [27], implying a more homogeneous core, which allowed more neutrons to slow down from fission energy to thermal energies and create a softer neutron spectrum, as shown in Fig. 4a–c. The energy of the average lethargy of fission

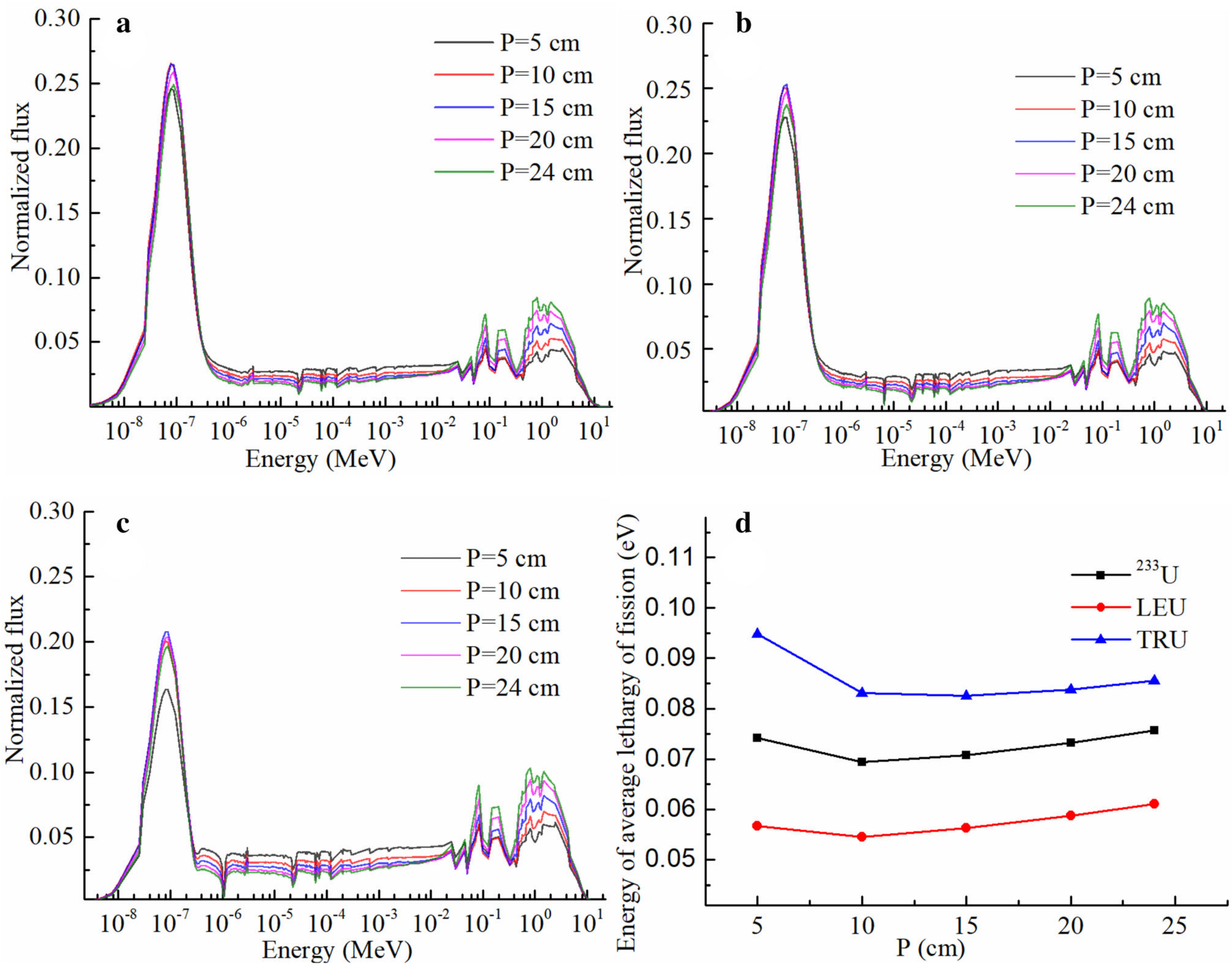

Fig. 4 (Color online) The neutron spectrum of **a** ^{233}U-Th starting, **b** LEU-Th starting, **c** TRU-Th starting reactor at different square size, and **d** energy of average lethargy of fission

(EALF) [28] is an important parameter to quantify the hardness of the neutron spectrum. It is weighted by the fission cross section and the neutron flux, reflecting the average energy level of the fission reaction caused by the entire neutron in the core. The higher the EALF, the harder spectrum to be obtained, and vice versa. The EALFs of the three fuels are shown in Fig. 4d. At a given P value, TRU-Th fuel exhibits the hardest neutron spectrum, while the neutron spectrum is the softest for the LEU-Th fuel. This was mainly caused by the different resolved resonance energies of heavy metal nuclides in different fuels. The main resolved resonances of the isotopes for fertile nuclide absorption and fissile nuclide fission are shown in Table 3. In addition, the fractions of thorium in the three mixtures differed because the molar fraction of heavy nuclide remained constant (12.3 mol%) and the presence of fertile nuclides ^{238}U and ^{240}Pu in respective LEU-Th and TRU-Th fuel correspondingly decreased the ^{232}Th fractions in these two fuels. Because the resolved resonance absorption energies of ^{240}Pu and ^{239}Pu from TRU-Th fuel were closer to the neutron spectrum peak in the thermal energy region compared with the nuclides from ^{233}U-Th and LEU-Th fuel, more thermal neutrons were absorbed by TRU-Th fuel, hardening the neutron spectrum of TRU-Th fuel. For LEU-Th, the resonance energy of ^{238}U is lower than that of ^{232}Th, lower-energy neutron absorption was greater compared with ^{233}U-Th fuel. This is a negative effect, softening the neutron spectrum of LEU-Th fuel compared with that of ^{233}U-Th fuel. However, the resonance energy of ^{235}U is

Table 3 The resolved resonance energy (E_r)

Fertile nuclide	E_r (eV)	Fissile nuclide	E_r (eV)
^{232}Th	22	^{235}U	5
^{238}U	8	^{233}U	2
^{240}Pu	1	^{239}Pu	0.3

higher than ^{233}U, which causes higher energy neutrons to be absorbed, and this is a positive effect resulting in a softer neutron spectrum for LEU-Th fuel. The aforementioned effects competed with each other and led to the lowest EALF (the softest neutron spectrum) for the LEU-Th fuel. In addition, Fig. 4d shows that the EALF first decreased and then increased for all three fuels, indicating that the neutron spectrum did not change monotonically with *P*. This mainly occurred due to the decrease in fissile loading and the homogeneity of the core as *P* increased. Because the molar ratio of heavy nuclides, LEU enrichment, and the fraction of each nuclide of TRU were assumed to be constant in this work, the decrease in fissile loading could have led to an increase in ^{232}Th loading when *P* increased (this is described in detail in Sect. 3.3). Because the ^{232}Th resonance energy was higher than that of other fertile or fissile nuclides (^{233}U, ^{235}U, ^{239}Pu, ^{240}Pu, ^{238}U), more thermal neutrons remained, which softened the neutron spectrum and decreased EALF. In contrast, as the *P* value increased, the heterogeneity of the core increased, and the neutron-moderating ability decreased, which hardened the neutron spectrum and increased EALF. The above two influences competed with each other, resulting in the EALF value of the three fuels decreasing at first and then increasing with the *P* value.

The influence of *VF* on the neutron spectrum is shown in Fig. 5a–c; the *P* value remained constant (*P* = 5 cm). For all three fuels, increasing *VF* weakened the moderating ability and hardened the neutron spectrum, resulting in an increase in EALF. Over the investigated *VF* range (4% to 28%), the neutron spectra of the cores were the thermal neutron spectra for the ^{233}U-Th and LEU-Th fuels. The neutron spectrum of the core loaded with TRU-Th fuel changed more significantly with *VF* (Fig. 5c). When *VF* was approximately 24%, the EALF increased rapidly (Fig. 5d), and the core became a fast neutron spectrum core as *VF* increased to more than 28%. This mainly occurred because the resonance energies of TRU isotopes were closer to the thermal energy compared with the other two fuels, which caused more thermal neutrons to be absorbed.

3.2 Conversion performance

CR is an important parameter used for measuring Th-^{233}U conversion performance that is affected by *P* and *VF*. A traditional *CR* definition can be expressed as [29]

$$CR = \frac{R_c\left({}^{232}\mathrm{T} + {}^{234}\mathrm{U} + {}^{238}\mathrm{U} + {}^{238}\mathrm{Pu} + {}^{240}\mathrm{Pu} - {}^{233}\mathrm{Pa}\right)}{R_a\left({}^{233}\mathrm{U} + {}^{235}\mathrm{U} + {}^{239}\mathrm{Pu} + {}^{241}\mathrm{Pu}\right)}, \tag{1}$$

where R_c represents the neutron capture reaction rate of fertile nuclides, *R*a is the neutron absorption reaction rate of fission nuclides, and ^{233}Pa on the numerator represents the loss of ^{233}U resulting from the neutron absorption of ^{233}Pa. To analyze the effects of geometrical parameters on *CR*, only the initial core was considered, and burnup was not involved. Hence, a simplified equation of *CR* without ^{233}Pa was adopted, and it can be calculated by [30, 31].

$$CR = \frac{R_c\left({}^{232}\mathrm{T} + {}^{234}\mathrm{U} + {}^{238}\mathrm{U} + {}^{238}\mathrm{Pu} + {}^{240}\mathrm{Pu}\right)}{R_a\left({}^{233}\mathrm{U} + {}^{235}\mathrm{U} + {}^{239}\mathrm{Pu} + {}^{241}\mathrm{Pu}\right)} \tag{2}$$

Fixing *P*, and increasing the *VF* hardens the neutron spectrum. The fission cross section of fissile nuclides declines faster than the capture cross section of fertile nuclides, generating a positive effect on enhancing the *CR*. In contrast, the hardening neutron spectrum increased the fissile nuclides loading because of the reduction in the fission cross section and decreased the loading of fertile nuclides because the molar ratio of heavy nuclides was fixed at 12.3 mol%, at which the *CR* was expected to deteriorate. In addition, a thermal insulator contains zirconium nuclide, which has a large neutron absorption cross section. Because the thickness of the thermal insulator was fixed at 3 mm, a change in the radius (*R*) of the thermal insulator could cause a variation in the volume fraction of the thermal insulator to the molten salt (*VF*(Zr)), which affects the *CR*. As shown in Fig. 6d (because the change trends of *VF* and *VF*(Zr) with *R* at different *P* values were consistent, only the case of *P* = 20 cm is demonstrated), the increasing *VF* made *R* and *VF*(Zr) increase and decrease, respectively, which in turn resulted in a decrease of zirconium nuclide and generated a positive effect on enhancing the CR. The above three effects competed with each other and determined the *CR* performance for ^{233}U-Th, LEU-Th, and TRU-Th loading scenarios. For ^{233}U-Th and LEU-Th fuel, in view of the slow change in the neutron spectrum and the competition among the above three effects, *CR* increased gradually with *VF* and then reached an equilibrium state (Fig. 6a, b). However, there is a rapid hardening of the neutron spectrum for TRU-Th fuel as *VF* increased to be larger than 12%, which led to a significant increase in TRU loading and a rapid decrease in thorium loading because the molar ratio of heavy metal nuclides was assumed to be constant. As a result, the *CR* decreased subsequently for the TRU-Th fuel.

When the *VF* was maintained and P varied from 24 to 10 cm, the core became more homogeneous and the neutron spectrum softened slightly (shown in Fig. 4d), in which the loading of fissile nuclides decreased and that of fertile nuclides subsequently increased. As a result, the *CR* decreased slightly. Due to the significant increase in *VF*(Zr), *CR* rapidly decreased as *P* varied from 10 to 4 cm. *CR* increased with *P* when *P* was greater than 15 cm, and the *CR* values for the three fuels are close to the maximum

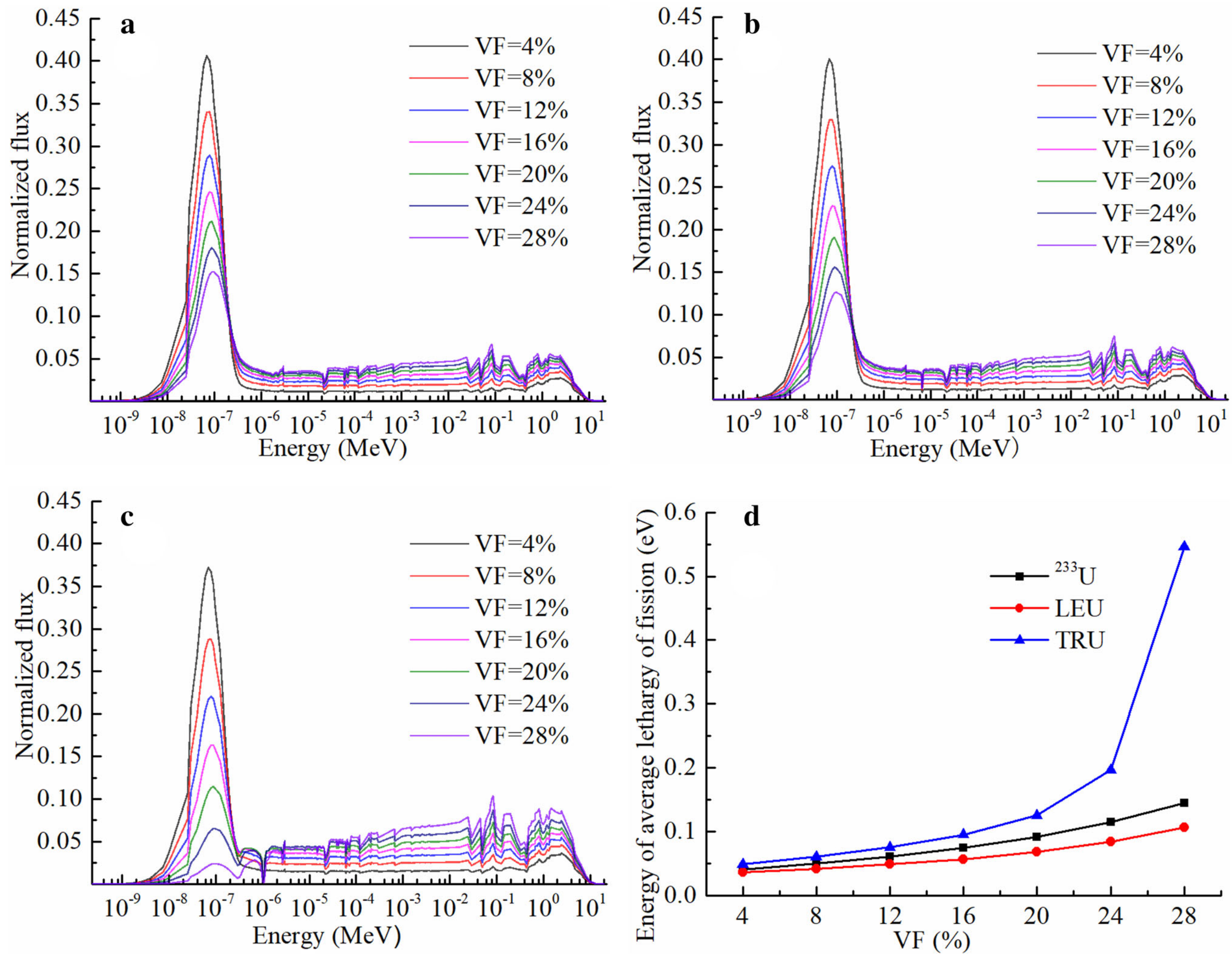

Fig. 5 (Color online) Neutron spectrum of **a** ^{233}U-Th starting, **b** LEU-Th starting, **c** TRU-Th starting at different VF, and **d** energy of average lethargy of fission

value: *CR* of ^{233}U-Th fuel is approximately 1.05, *CR* of LEU-Th fuel is approximately 0.87, and *CR* of TRU-Th fuel is approximately 0.78.

To obtain a higher *CR*, a larger *P* value must be selected for ^{233}U-Th and LEU-Th fuels, while a smaller *VF* must be chosen for the TRU-Th fuel. Specifically, the preferred ranges of *P* value and *VF* are 15–24 cm and 16–28% for ^{233}U-Th fuel, 15–24 cm and 16–24% for LEU-Th fuel, and 15–24 cm and 8–12% for TRU-Th fuel.

3.3 Initial fissile loading mass

Figure 7 shows the initial fissile loading of ^{233}U-Th, LEU-Th, and TRU-Th fuels at different *P* and *VF* values. At a given *P*, it can be seen that the fissile loading mass of ^{233}U-Th fuel decreased at first and then gradually increased with *VF*, while the fissile loading masses of LEU-Th (except *P* = 5 cm) and TRU-Th fuels presented a gradual increase over the *VF* from 4 to 28%. The phenomenon described above was the result of competition between the hardening neutron spectrum, which subsequently increased the initial fissile loading mass, and the decrease in *VF*(Zr) (less parasitic neutron absorption, Fig. 6d) that led to a reduction in the initial fissile loading mass as *VF* increased. At a given *VF*, increasing *P* softened and hardened the neutron spectrum successively, as shown in Fig. 4d, which caused the initial fissile loading mass to decrease and increase in succession. In addition, increasing *P* decreased *VF*(Zr), as depicted in Fig. 7d (it should be noted that only *VF* = 16% is demonstrated in Fig. 7d because the same change trends are presented for other *VF*s), resulting in a reduction of the initial fissile loading mass. Meanwhile, the initial fissile loading mass exhibited an obvious decrease as P increased from 5 to 10 cm, because the decrease in *VF*(Zr) is quite significant. When *P* further increased, the decrease in the initial fissile loading mass slowed and finally reached equilibrium, which resulted from the competition between the change in the neutron spectrum and

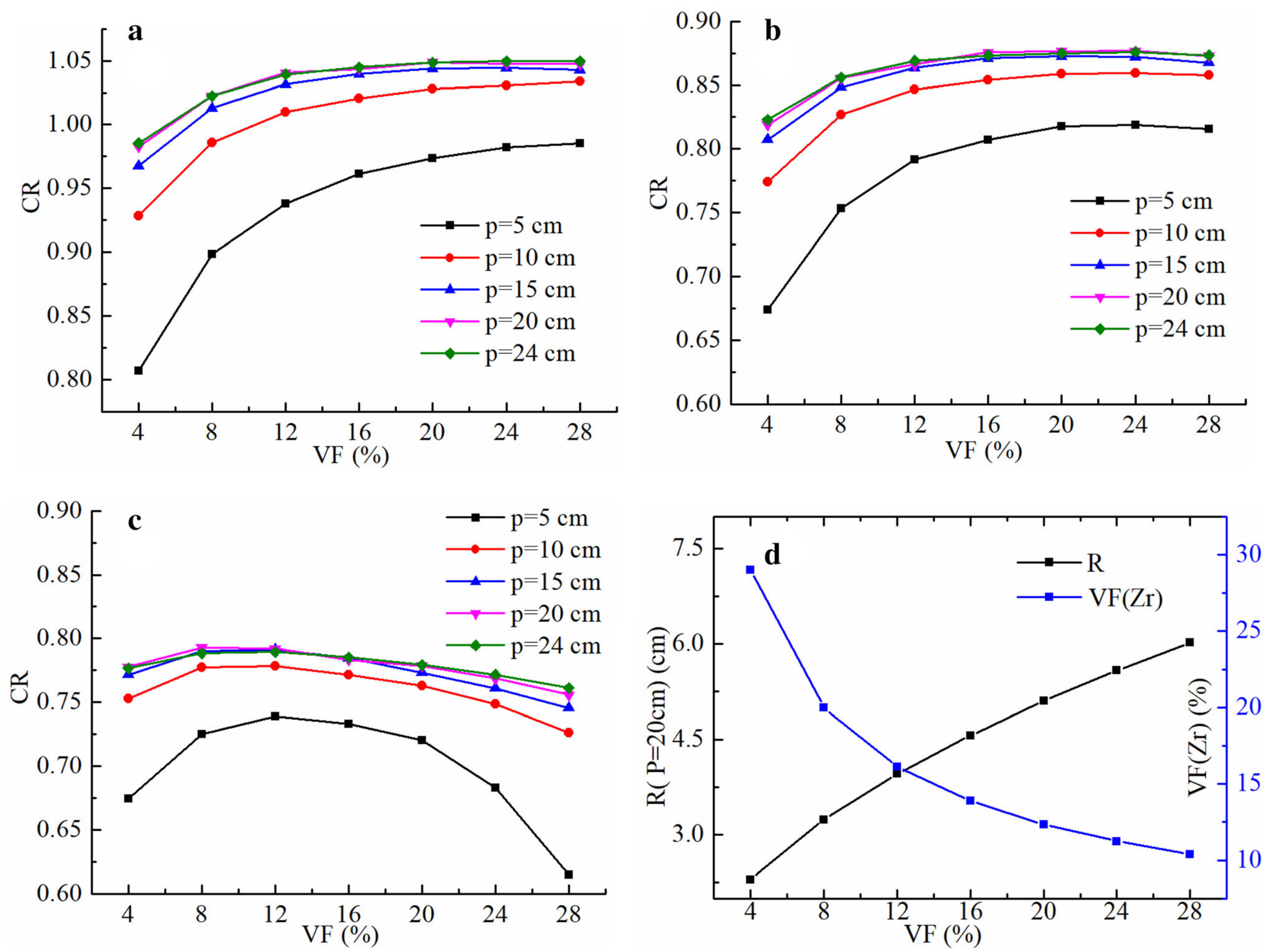

Fig. 6 (Color online) *CR* of three staring fuels and volume fraction of thermal insulator with *VF*: **a** ^{233}U-Th, **b** LEU-Th, **c** TRU-Th, **d** *VF*(Zr) with VF

the decrease in *VF*(Zr). For TRU-Th fuel, a rapid fissile loading mass increase was incited by increasing the *VF* from 20 to 28% at a P of 5 cm. This was mainly because the thermal neutron spectrum gradually shifted to the epithermal and fast spectrum (Fig. 5c), which resulted in a resonance absorption of heavy elements at epithermal neutron spectrum as well as the rapid reduction of fission cross section at a fast neutron spectrum.

To achieve a lower fissile loading mass, from the above results, one can conclude that the preferred selection ranges of *P* and *VF* are 20–24 cm and 8–12% for ^{233}U-Th fuel, 15–24 cm and 4–8% for LEU-Th fuel, and 10–24 cm and 8–12% for TRU-Th fuel.

3.4 Temperature coefficient

To ensure that the reactor is intrinsically safe, the temperature coefficient must be negative. For the SM-HWMSR, the moderator and fuel salt are separated by a thermal insulator, causing a change in the moderator temperature lag behind the variation in the fuel salt temperature. Hence, the temperature feedback performance of the fuel salt and moderator should be analyzed separately. The fuel salt temperature coefficient can be decomposed into two components, that is, density coefficient and Doppler coefficient [11, 32]:

$$\left(\frac{\mathrm{d}k}{\mathrm{d}T}\right)_{\text{fuel total}} = \left(\frac{\mathrm{d}k}{\mathrm{d}T}\right)_{\text{fuel density}} + \left(\frac{\mathrm{d}k}{\mathrm{d}T}\right)_{\text{doppler}}. \tag{3}$$

The density coefficient results from the volume expansion of the fuel salt due to the temperature increment. On the one hand, overflowed fuel salt from the core will lead to the reduction of fissile nuclide inventory and subsequently decrease the fission reaction rate and improve the fuel density coefficient. On the other hand, reduced fuel salt in the core will soften the neutron spectrum and increase the fission reaction rate, deteriorating the density coefficient. These two effects competed with each other and determined the density coefficient. When *VF* increased, the neutron spectrum hardened, and the effect of neutron

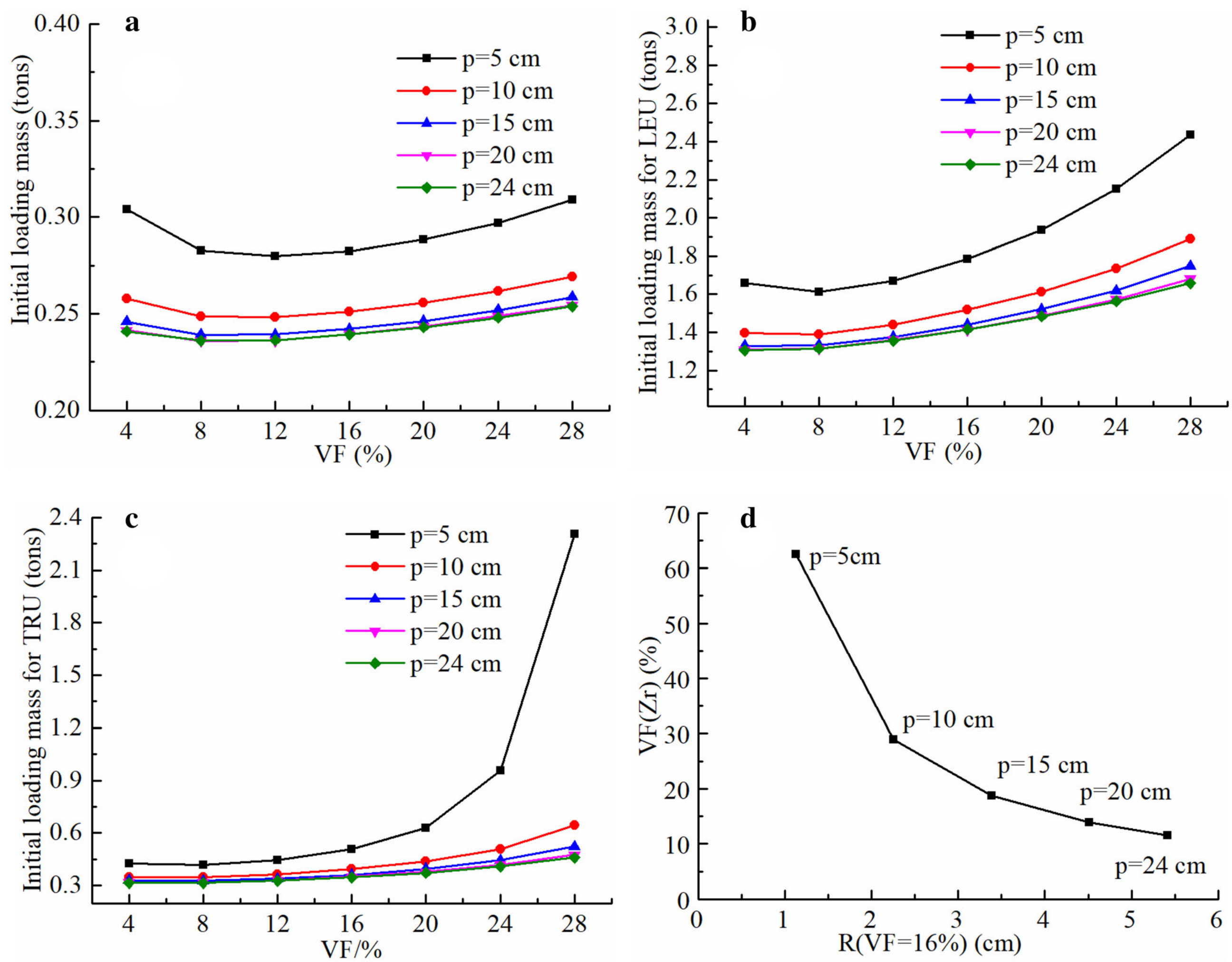

Fig. 7 (Color online) Initial loading mass of three staring fuels and volume fraction of thermal insulator with R: **a** ^{233}U-Th, **b** LEU-Th, **c** TRU-Th, and **d** *VF*(Zr) with *R*

spectrum softened by the reduced fuel salt on the fuel density coefficient became more significant. As a result, the fuel density coefficient worsened with the *VF*, as shown in Fig. 8a. In addition, ^{233}U-Th fuel has the least fissile loading mass compared with LEU-Th and TRU-Th fuels with the same core parameters. The small fissile loading mass can result in a greater relative reduction with the same overflowed fuel salt, thus resulting in a greater decrease in the fission reaction rate, leading to a preferable fuel density coefficient for ^{233}U-Th fuel.

The Doppler coefficient (Fig. 8b) results from the effect of resonance broadening when the fuel temperature increases [10]. Because the fission resonance energy of the fissile nuclide was closer to the thermal energy than the resonance absorption of the fertile nuclide, the resonance fission rate of fissile nuclide decreased more significantly as *VF* increased, which hardened the neutron spectrum and led to a more negative Doppler coefficient. Compared with ^{233}U-Th and LEU-Th fuels, the resonance energy (0.3 eV) of ^{239}Pu and ^{241}Pu in TRU-Th fuel was closer to the thermal energy than ^{233}U (2 eV) and ^{235}U (5 eV). More thermal neutrons are absorbed by ^{239}Pu and ^{241}Pu for fission when the fuel temperature increases, leading to a relatively poor Doppler coefficient for TRU-Th fuel compared with the other two fuels.

The temperature coefficient of the fuel salt is the sum of the density coefficient and Doppler coefficient, as shown in Fig. 8c. A negative temperature coefficient could be obtained for ^{233}U-Th and LEU-Th fuels over the investigated range of *P* and *VF*, while the value of P was expected to be less than 5 cm to ensure a negative temperature coefficient for TRU-Th fuel, mainly because of the poor Doppler coefficient. In summary, the preferred selection ranges of *P* and *VF* are 5–24 cm and 4–24% for ^{233}U-Th fuel, 5–10 cm and 4–28% for LEU-Th fuel, and 5 cm and 4%, 24–28% for TRU-Th fuel, respectively.

The density of the moderator decreased as the temperature increased. The decreasing density of the moderator

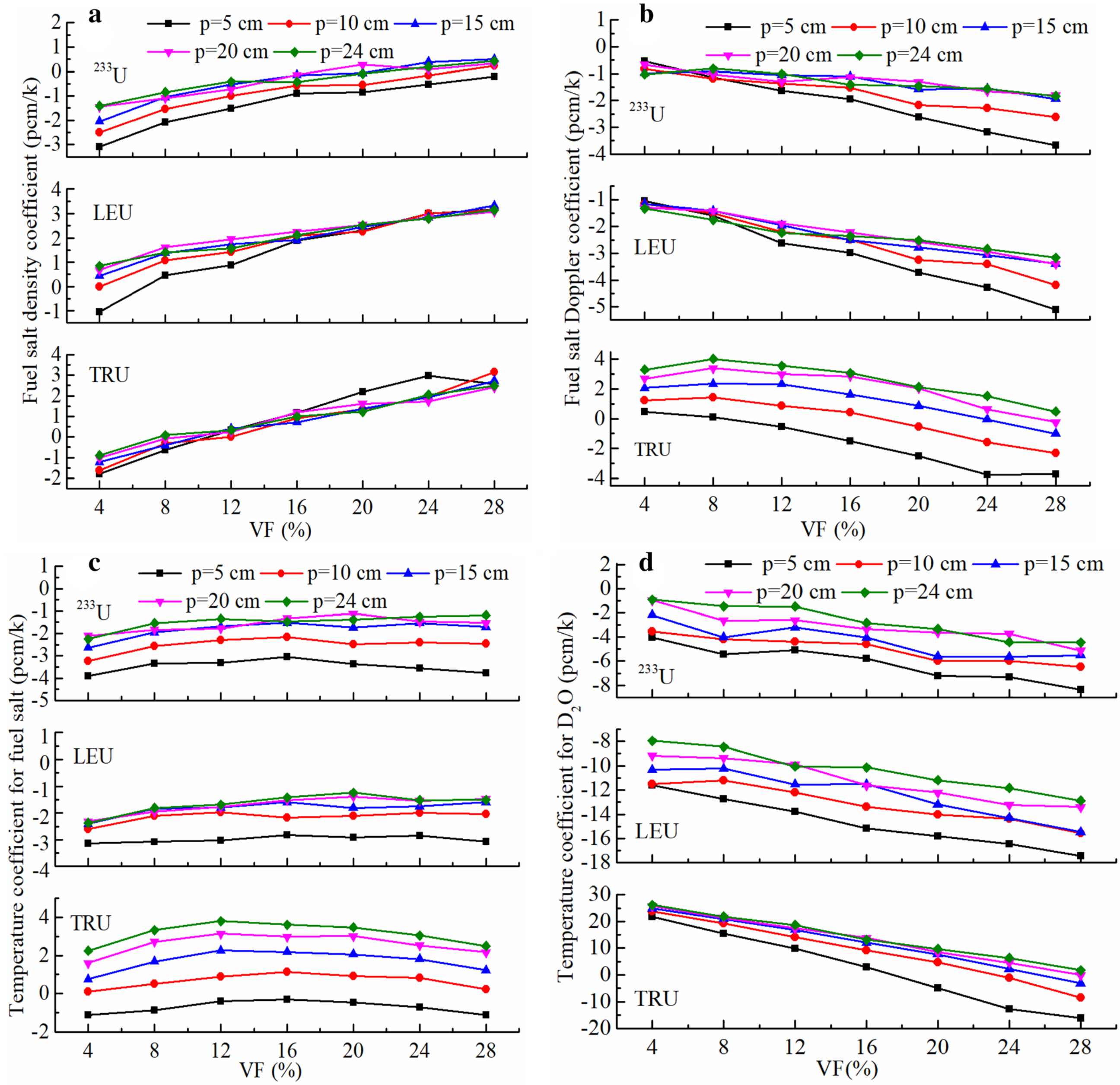

Fig. 8 (Color online) Temperature coefficient for **a** fuel salt density coefficient, **b** Doppler coefficient, **c** fuel salt, and **d** D_2O

hardened the neutron spectrum and raised the neutron leakage, which can reduce the fission reaction rate and improve the temperature coefficient of heavy water. In contrast, the decreasing density of the moderator can decrease the neutron parasitic absorption, leading to an increase in the fission reaction rate and deteriorating the temperature coefficient of heavy water. At a small *VF*, the core is mainly filled with heavy water, and the reduction of parasitic absorption plays an important role. When *VF* increases, the core becomes more undermoderated in which the hardening neutron spectrum and the increase in neutron leakage dominate, subsequently obtaining a more negative temperature coefficient of heavy water (Fig. 8d). In addition, increasing the temperature of the moderator can shift the Maxwell spectrum to higher energy regions, which is propitious to fission of fissile nuclide over the neutron capture of fertile nuclides, in which the temperature coefficient of heavy water worsens. The effect of this shift is more obvious for the Doppler coefficient of TRU-Th fuel because the resolved resonances for ^{239}Pu and ^{241}Pu fission in TRU are closer to the thermal energy than the other two fuels, in which the core reactivity increases more significantly, further deteriorating the temperature coefficient. Compared with TRU-Th fuel, the resolved resonances for

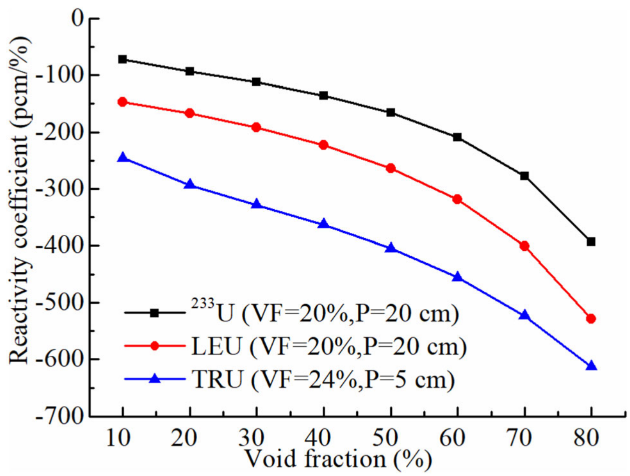

Fig. 9 (Color online) Heavy water moderator void coefficient

^{233}U and ^{235}U fission are higher; therefore, the shift of the Maxwell spectrum has less impact, resulting in a negative temperature coefficient of heavy water with P and VF in the investigated ranges, that is, 5–24 cm and 4–28%, respectively.

4 Preferred core geometrical parameters for three fuels

By balancing the performance of the initial *CR*, the initial fissile loading mass and temperature coefficient, *P* and *VF* values, respectively, of 20 cm and 20% for ^{233}U-Th fuel, 20 cm and 20% for LEU-Th fuel, 5 cm and 24% for TRU-Th fuel are recommended (shown in Table 4).

For ^{233}U-Th fuel, the initial *CR* can achieve 1.048 with an initial ^{233}U loading mass of 0.24 tons, and the fuel salt and moderator temperature coefficients are − 1.125 pcm/K and − 3.635 pcm/K, respectively. The preferred CR and initial fissile loading mass of LEU in LEU-Th fuel are obtained, which are 0.876 and 1.47 tons, respectively. The fuel salt and moderator temperature coefficients can achieve − 1.37 pcm/K and − 12.10 pcm/K, respectively. For TRU-Th fuel, the initial CR and initial fissile loading mass of TRU in TRU-Th fuel are 0.683 and 0.96 tons, respectively, and the fuel salt and moderator temperature coefficients are − 0.58 pcm/K and − 12.875 pcm/K, respectively.

For the recommended geometrical parameters, the void coefficients for the three fuels are evaluated because moderator boiling may occur for SM-HWMSR in an accident. As shown in Fig. 8, the void coefficients are all negative for the three fuels because an increasing void fraction will lead to a decrease in the moderator volume, which can further harden the neutron spectrum and reduce the fission reaction rate, making the void coefficient more negative. Because the neutron spectrum of TRU-Th fuel was harder and changed faster with *VF* than ^{233}U-Th and LEU-Th fuels, its void coefficient is more negative.

Table 4 Preferred geometrical parameters and initial fuel cycle performances

Fuel	*P* (cm)	*VF* (%)	*CR*	Fissile fuel/Th loading mass (tons)	Fuel salt/moderator temperature coefficient (pcm/K)
^{233}U	20	20	1.048	0.24/18.1	− 1.125/ − 3.635
LEU	20	20	0.876	1.47/16.8	− 1.37/ − 12.10
TRU	5	24	0.683	0.96/17.3	− 0.58/ − 12.875

5 Conclusion

In this study, the preliminary fuel cycle performances of an SM-HWMSR with three starting fuels, ^{233}U-Th, LEU-Th, and TRU-Th fuels, were investigated by varying *P* and *VF*, respectively, from 5 to 24 cm and from 4 to 28%, respectively, to cover the potential core structures under the thermal neutron spectrum. According to the obtained results, the preferred core geometrical parameters for each fuel loading scenario were selected. For ^{233}U-Th fuel, the initial *CR* increased and gradually reached equilibrium as *P* and *VF* increased. Its initial fissile loading mass decreased and gradually reached equilibrium as *P* increased, while, as *VF* increased, the initial fissile loading mass declined and subsequently increased. The temperature coefficient was negative for all investigated core models with various *P* and *VF* values. For the LEU-Th fuel, the change trends of the initial *CR*, initial fissile loading mass, and temperature coefficient with *P* and *VF* were consistent with ^{233}U-Th. A core with *P* of 20 cm and *VF* of 20% was recommended for ^{233}U-Th and LEU-Th fuel, in which CR could achieve 1.048 and 0.876, respectively. The initial ^{233}U loading and LEU loading were 0.24 tons and 1.47 tons, respectively. For TRU-Th fuel, small *P* and large *VF* were required to obtain a negative temperature coefficient. A core with a *P* value of 5 cm and a *VF* of 24% is recommended, in which *CR* and the initial TRU loading are 0.683 and 0.96 tons, respectively. Moreover, the recommended cores for the three fuels have a negative void coefficient.

In addition, the initial conversion ratios of LEU-Th and TRU-Th fuels are less than 1 and cannot achieve fuel breeding. However, an extra ^{233}U can be obtained through online extraction of ^{233}Pa while feeding LEU and TRU during the operation time. By taking this approach, the amount of ^{233}U used to restart a new SM-HWMSR core is expected to be quickly obtained and the transition to thorium fuel cycle can be realized. The scheme of thorium fuel cycle transition using LEU-Th and TRU-Th fuels will be further discussed in the future.

Further studies should be considered on developing better insulation between the heavy water moderator and the fuel salt, for example, a pressure tube/calandria tube concept with a CO_2 gas gap. In addition, the organic compound, deuterated diphenyl ($C_{12}D_{10}$), with a high boiling point at $\sim$ 230 °C (at 1 atm) can be selected as an alternative to heavy water. The fission energy deposited into the moderator caused by neutrons slowing down heats $C_{12}D_{10}$ to generate steam for a higher overall plant efficiency. Meanwhile, a two-fluid two-zone core design with the "seed" region containing PuF_3/ThF_4 fuel salt, and the "blanket region" with ThF_4 mixed with AmF_4/CmF_4 could be an attractive design to enhance fuel breeding.

References

1. U.S. DOE. A technology roadmap for generation IV nuclear energy systems, Philos. Rev. **66**(2), 239–241 (2002). https://doi.org/10.2172/859029
2. T. Abram, S. Ion, Generation-IV nuclear power: a review of the state of the science. Energy Policy **36**(12), 4323–4330 (2008). https://doi.org/10.1016/j.enpol.2008.09.059
3. J. Serp, M. Allibert, O. Benes et al., The molten salt reactor (MSR) in generation IV: overview and perspectives. Prog. Nucl. Energy **77**, 308–319 (2014). https://doi.org/10.1016/j.pnucene.2014.02.014
4. P.N. Haubenreich, J.R. Engel, Experience with the molten-salt reactor experiment. Nucl. Eng. Technol. **8**(2), 118–136 (1970). https://doi.org/10.13182/NT8-2-118
5. M.W. Rosenthal, P.R. Kasten, R.B. Briggs, Molten-salt reactors—history, status, and potential. Nucl. Eng. Technol. **8**(2), 107–117 (1970). https://doi.org/10.13182/NT70-A28619
6. H.G. MacPherson, The molten salt reactor adventure. Nucl. Sci. Eng. **90**(4), 374–380 (1985). https://doi.org/10.13182/NSE90-374
7. M.E. Whatley, L.E. McNeese, W.L. Carter et al., Engineering development of the MSBR fuel recycle. Nucl. Eng. Technol. **8**(2), 170–178 (1970). https://doi.org/10.13182/NT70-A28623
8. R. C. Robertson, Conceptual Design Study of a Single-Fluid Molten-Salt Breeder Reactor, United States, Technical Report, ORNL-4541 (1971). https://doi.org/10.2172/4030941
9. J. Krepel, U. Rohde et al., Dynamics of molten salt reactors. Nucl. Technol. **164**(1), 34–44 (2008). https://doi.org/10.13182/NT08-A4006
10. A. Nuttin, D. Heuer, A. Billebaud et al., Potential of thorium molten salt reactors detailed calculations and concept evolution with a view to large scale energy production. Prog. Nucl. Energy **46**(1), 77–99 (2005). https://doi.org/10.1016/j.pnucene.2004.11.001
11. L. Mathieu, D. Heuer, R. Brissot et al., The thorium molten salt reactor: moving on from the MSBR. Prog. Nucl. Energy. **48**(7), 664–679 (2006). https://doi.org/10.1016/j.pnucene.2006.07.005
12. L. Mathieu, D. Heuer, E. Merle-Lucotte et al., Possible configurations for the thorium molten salt reactor and advantages of the fast nonmoderated version. Nucl. Sci. Eng. **161**(1), 78–89 (2009). https://doi.org/10.13182/NSE07-49
13. G.C. Li, Y. Zou, C.G. Yu et al., Model optimization and analysis of Th-U breeding based on MSFR. Nucl. Tech. **40**(2), 020603 (2017). https://doi.org/10.11889/j.0253-3219.2017.hjs.40.020603 **(in Chinese)**
14. D.G. Li, G.M. Liu, Analysis of Th-U breeding in molten salt fast reactor. Nucl. Tech. **43**(5), 050604 (2020). https://doi.org/10.11889/j.0253-3219.2020.hjs.43.050604 **(in Chinese)**
15. J. Zhou, J.G. Chen, C.G. Yu et al., Influence of 7Li enrichment in FLi/FLiBe on Th-U conversion performance. Nucl. Tech. **42**(11), 110601. https://doi.org/10.11889/j.0253-3219.2019.hjs.42.110601 **(in Chinese)**
16. J. H. Wu, J. G. Chen J, X. Z. Kang et al. A novel concept for a molten salt reactor moderated by heavy water, Ann. Nucl. Energy **132**, 391–403 (2019). https://doi.org/10.1016/j.anucene.2019.04.043
17. S. Delpech, E. Merle-Lucotte, D. Heuer et al., Reactor physic and reprocessing scheme for innovative molten salt reactor system. J. Fluorine Chem. **130**(1), 11–17 (2009). https://doi.org/10.1016/j.jfluchem.2008.07.009
18. V. Ignatiev, O. Feynberg, I. Gnidoi et al., Molten salt actinide recycler and transforming system without and with Th–U support: Fuel cycle flexibility and key material properties. Ann. Nucl. Energy **64**, 408–420 (2014). https://doi.org/10.1016/j.anucene.2013.09.004
19. R.J. Sheu, C.H. Chang, C.C. Chao et al., Depletion analysis on long-term operation of the conceptual Molten Salt Actinide Recycler & Transmuter (MOSART) by using a special sequence based on SCALE6/TRITON. Ann. Nucl. Energy **53**, 1–8 (2013). https://doi.org/10.1016/j.anucene.2012.10.017
20. V. Nian, J. Bauly, Nuclear Power Developments: Could small modular reactor power plants be a "game changer"? - The ASEAN perspective, ICAE2014, **61**, 17–20 (2014). https://doi.org/10.1016/j.egypro.2014.11.895
21. H.R. Trellue, R.J. Kapernick, D.V. Rao et al., Salt-cooled modular innovative thorium heavy water-moderated reactor system. Nucl. Technol. **182**(1), 26–38 (2012). https://doi.org/10.13182/NT13-A15823
22. K. Sasaki, T. Terai, A. Suzuki et al., Effect of the Y_2O_3 Concentration in YSZ on the thermophysical property as a thermal shielding material. Int. J. Appl. Ceram. Technol. **7**(4), 518–527 (2010). https://doi.org/10.1111/j.1744-7402.2009.02363.x
23. J.Y. Park, SiCf/SiC composites as core materials for Generation IV nuclear reactors. Struct. Mater. Gener. IV Nucl. React **106**, 441–470 (2017). https://doi.org/10.1016/B978-0-08-100906-2.00012-4
24. R. Scarlat, M. Laufer, E. Blandford et al., Design and licensing strategies for the fluoride-salt-cooled, high-temperature reactor (FHR) technology. Prog. Nucl. Energy **77**, 406–420 (2014). https://doi.org/10.1016/j.pnucene.2014.07.002
25. G.C. Li, Y. Zou, C.G. Yu et al., Influences of Li-7 enrichment on Th-U fuel breeding for an Improved Molten Salt Fast Reactor (IMSFR). Nucl. Sci. Tech. **28**(7), 97 (2017). https://doi.org/10.1007/s41365-017-0250-7
26. C.Y. Zou, C.Z. Cai, C.G. Yu et al., Transition to thorium fuel cycle for TMSR. Nucl. Eng. Des. **330**, 420–428 (2018). https://doi.org/10.1016/j.nucengdes.2018.01.033
27. J. Duderstadt, L. Hamilton, *Nuclear Reactor Analysis* (Wiley, Hoboken, 1976)
28. X.X. Li, D.Y. Cui, Y.W. Ma et al., Influence of ^{235}U enrichment on the moderator temperature coefficient of reactivity in a graphite-moderated molten salt reactor. Nucl. Sci. Tech. **30**(11), 166 (2019). https://doi.org/10.1007/s41365-019-0694-z
29. X.C. Zhao, D.Y. Cui, X.Z. Cai et al., Analysis of Th-U breeding capability for an accelerator-driven subcritical molten salt reactor. Nucl. Sci. Tech. **29**, 121 (2018). https://doi.org/10.1007/s41365-018-0448-3

30. L.Y. He, S.P. Xia, R. Yan et al., Th-U and U-Pu cycling performances of molten chloride salt fast reactor under LEU start-up mode. Nucl. Tech. **43**(1), 010604 (2020). https://doi.org/10.11889/j.0253-3219.2020.hjs.43.010604 **(in Chinese)**
31. G.C. Li, P. Cong, C.G. Yu et al., Optimization of Th-U fuel breeding based on a single-fluid double-zone thorium molten salt reactor. Prog. Nucl. Energy **108**, 144–151 (2018). https://doi.org/10.1016/j.pnucene.2018.04.017
32. X.X. Li, Y.W. Ma, C.G. Yu et al., Effects of fuel salt composition on fuel salt temperature coefficient (FSTC) for an under-moderated molten salt reactor (MSR). Nucl. Sci. Tech. **29**(8), 110 (2018). https://doi.org/10.1007/s41365-018-0458-1

Publisher's Note